Karlsruhe Institute of Technology

Bandwidth-Efficient Parallel Visualization for Mobile Devices

A. Helfrich-Schkarbanenko, V. Heuveline, R. Reiner,
S. Ritterbusch

No. 2012-07

Preprint Series of the Engineering Mathematics and Computing Lab (EMCL)

KIT – University of the State of Baden-Wuerttemberg and
National Research Center of the Helmholtz Association

www.emcl.kit.edu

Preprint Series of the Engineering Mathematics and Computing Lab (EMCL)
ISSN 2191–0693
No. 2012-07

Impressum

Karlsruhe Institute of Technology (KIT)
Engineering Mathematics and Computing Lab (EMCL)

Fritz-Erler-Str. 23, building 01.86
76133 Karlsruhe
Germany

KIT – University of the State of Baden Wuerttemberg and
National Laboratory of the Helmholtz Association

Bandwidth-Efficient Parallel Visualization for Mobile Devices

Andreas Helfrich-Schkarbanenko, Vincent Heuveline, Roman Reiner, Sebastian Ritterbusch
Engineering Mathematics and Computing Lab (EMCL)
Karlsruhe Institute of Technology (KIT)
Karlsruhe, Germany
{*andreas.helfrich-schkarbanenko, vincent.heuveline, roman.reiner, sebastian.ritterbusch*}@*kit.edu*

***Abstract*—For visual analysis of large numerical simulations on mobile devices, we introduce a remote parallelizable visualization method for low-bandwidth and high-latency networks. Based on a mathematical model for multi-layered planar impostor representation of arbitrary complex and unbounded scenes, we derive optimal impostor placement from a derived metric. Using stochastic usage models, we prove the optimal bandwidth consumption order for choosing corresponding viewport impostor sets, leading to bandwidth-efficient remote visualization concepts for high performance computing simulation results.**

***Keywords*-**

I. Introduction

Remote visualization becomes vital wherever local storage, data transfer rates or graphical capabilities are limited. Even though the capabilities of modern smart phones are staggeringly increasing, many desirable applications are impeded by current hardware.

Image-based rendering techniques are widely used to reduce the geometric complexity of virtual environments by replacing parts of a scene with a textured representation approximating the original geometry.

Since these so-called *impostors* have a significantly simplified geometry, parallax errors occur on rendering the approximation. An impostor is generated for an initial *viewport* (that is, a position and viewing direction) and is said to be *valid* as long as the visual difference to the (hypothetically rendered) original geometry is below a certain threshold.

In our application these impostors are rendered remotely on render servers and streamed to a mobile device where they are used to approximate the scene. One substantial advantage of the impostor approach is, that the render time on the device only depends on the number of impostors and the resolution of the textures, not on the amount of data they display. As long as servers can generate and transfer the impostor textures sufficiently fast, every scene can be displayed remotely, regardless of its actual complexity. In this setting, network bandwidth is the bottleneck and a careful analysis of bandwidth consumption becomes mandatory.

We develop a mathematical model that allows to quantize the display error and propose an approximation method that proves to be optimal with respect to the derived error metric. We can show, that our method significantly reduces the total amount of image data that needs to be transferred. The key aspects of our method are illustrated in Figure I.1.

II. Related work

A variety of image-based rendering techniques are reviewed in [1] and [2]. The first paper focuses mainly on techniques using planar impostors but also mentions more exotic approaches like depth images (planar impostors with per-pixel depth information) and light fields. These and other techniques like view morphing and view dependent textures are examined in more detail in the second paper.

In the majority of cases planar impostors stacked with increasing distance to the observer are used [3], [4], [5], usually to approximate distant scene parts or single objects. In contrast, our approach uses impostors to represent the full scene.

For large objects, different parts of continuous surfaces can end up on different impostors which makes them tear apart when viewed from a shallow angle. Avoiding this particular problem was one focus of the method developed in [3]. Another interesting use of planar impostors is [6] where the authors render volume data on mobile phones.

Several approaches using geometrically more complex impostors can be found in [7], [8], [5]. In [1, Section 3.3] so-called *billboard clouds* are used to approximate the shape of an object using several intersecting planar impostors. While the impostor creation process for this approach is quite costly, the result allows examination from different viewing directions.

A very current example is Street Slide [9] which was presented at SIGGRAPH 2010 Street Slide sticks photos of front facades of urban environments to “panorama strips” that can be browsed by sliding sideways.

The need for accurate analysis of bandwidth and accuracy estimates, is discussed in [4], [1] without further specifying how to choose which viewports to load. A more in-depth analysis on the subject of pre-fetching is given in [10] and [11]. The former defines a so-called benefit integral indicating which parts of the scene – quality-wise – contribute most to the final image, the latter deals with rendering an indoor scene remotely. The task of remote rendering on mobile devices is addressed in [12] and [13], mostly focusing on the technical aspects of the server-client communication.

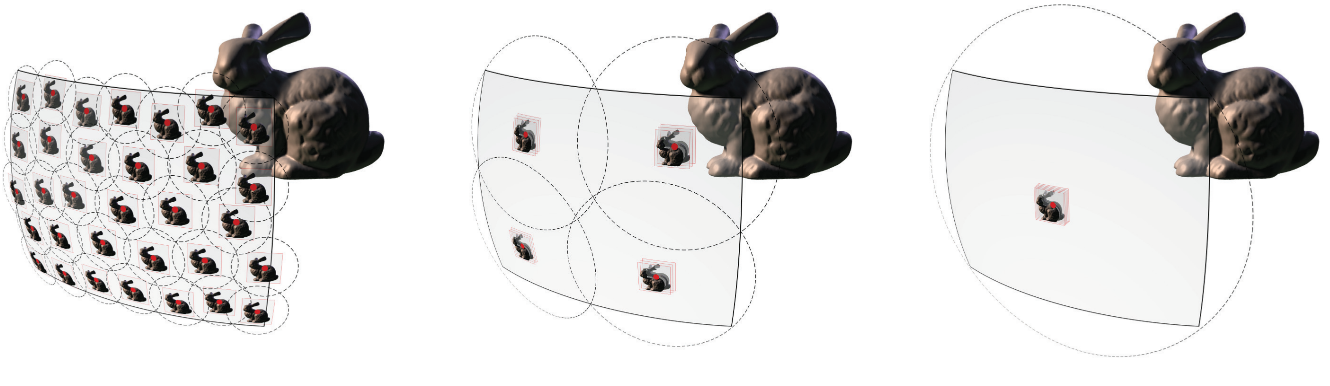

(a) 32 impostor sets with one layer each (b) Four impostor sets with three layers each (c) One impostor set with five layers

Figure I.1. An impostor representation is only valid inside a small region around the initial viewport for which it has been originally created. For observer viewports within this validity region (indicated by the dotted line) the display error does not exceed a given maximum value. To faithfully approximate the scene for all observer viewports inside the shaded area, several impostor sets have to be transmitted.
The validity regions can be enlarged (while keeping the maximum error unaltered) by increasing the number of layers per impostor set. As the number of required impostor sets drops faster than the number of layers per set increases, this significantly reduces the total number of layers needed to approximate the scene within the given error.

Usually, depending on the complexity of the approximation, an impostor is either easy to generate but only valid inside a small region and thus needs to be updated very often, or it is valid inside a large domain but complex and difficult to generate and display [2]. Since the former strains bandwidth and the latter strains render speed, any image-based rendering approach is usually a trade-off between the available capacities.

III. Visualization model and error metrics

To begin with, a mathematical model describing viewports and projections thereon needs to be established, with which the rendering and approximation processes can be described. This yields an error function describing the maximum parallax error of a scene as a function of the observer movement, called *domain error*.

Finally, building the observer movement as a probability distribution, we can describe the expected value of this error. This *interaction error* will be the cost function that we intend to minimize.

A. Perspective projection

Using homogeneous coordinates and projective transformations [14], we can express perspective projection as a 4×4 matrix multiplication on the projective space $\mathbb{P}^3$:

Definition III.1. The perspective projection onto the plane $x_3 = d$ towards the origin is a function

$$\pi_d : \left\{ \begin{array}{ccc} \mathbb{P}^3 \backslash \{(0,0,0,1)^\top\} & \longrightarrow & \mathbb{P}^3 \\ x & \longmapsto & P_d x \end{array} \right.$$

with the parameter $d > 0$ defining the proximity of the projection plane.

From the intercept theorems one can easily see that the perspective projection of a point $v = (v_1, v_2, v_3)^\top \in \mathbb{R}^3$, $v_3 \neq 0$ onto the plane $x_3 = d$ is given by $(\frac{d}{v_3} v_1, \frac{d}{v_3} v_2, d)^\top$ which, using homogeneous coordinates, equals $(v_1, v_2, v_3, \frac{v_3}{d})^\top$. This yields the projection matrix

$$P_d := \left(\begin{array}{ccc|c} 1 & 0 & 0 & 0 \\ 0 & 1 & 0 & 0 \\ 0 & 0 & 1 & 0 \\ \hline 0 & 0 & {}^1\!/\!{}_d & 0 \end{array} \right).$$

B. Viewports

Any viewport can be described by five values $c_1, c_2, c_3 \in \mathbb{R}$, $\vartheta \in [-\pi/2, \pi/2]$, $\varphi \in [-\pi, \pi)$, defining an affine transformation χ, which is the combination of a translation by the vector $(c_1, c_2, c_3)^\top$ followed by a rotation around the x_1-axis with the angle ϑ and a rotation around the x_2-axis with the angle φ (cf. Figure III.1). Actually there is a sixth value which represents a rotation around the viewing direction. Such a rotation, however, does not change the image besides rotating it. We assume the rotation to be lossless, which is why we do not need it for our purposes.

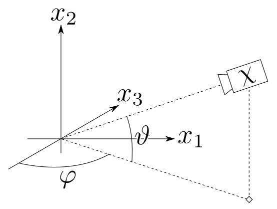

Figure III.1. The angles φ and ϑ of a viewport χ

We condense all five values into a single vector $c := (c_1, c_2, c_3, \vartheta, \varphi)^\top$. When describing viewports, we will use this vector c and the associated transformation χ_c interchangeably. In particular, we will identify sets of viewports with subsets of $\mathbb{R}^5$:

Definition III.2. The set

$$X := \mathbb{R}^3 \times [-\pi/2, \pi/2] \times [-\pi, \pi) \subset \mathbb{R}^5$$

will be called *viewport set*. For all practical purposes, however, we want to restrict to viewports inside a given set of *feasible viewports* $\Lambda \subset X$.

Projective matrix representations of χ_c and its inverse are

$$Q_c = \left(\begin{array}{c|c} B_{\vartheta,\varphi} & B_{\vartheta,\varphi}c \\ \hline 0 & 1 \end{array}\right) \quad \text{and} \quad Q_c^{-1} = \left(\begin{array}{c|c} B_{\vartheta,\varphi}^\top & -c \\ \hline 0 & 1 \end{array}\right)$$

where

$$B_{\vartheta,\varphi} := \begin{pmatrix} \cos\varphi & -\sin\varphi\sin\vartheta & -\sin\varphi\cos\vartheta \\ 0 & \cos\vartheta & -\sin\vartheta \\ \sin\varphi & \cos\varphi\sin\vartheta & \cos\varphi\cos\vartheta \end{pmatrix}.$$

We can now calculate a matrix representation of a projection onto an arbitrary viewport, by combining the matrices above with the matrix representations of the default projection π_d.

Definition III.3. Let χ be a viewport with an associated matrix representation Q and let π_χ denote a projection onto the viewport χ. Then, a matrix representation of π_χ is given by $P_{\chi,d} = QP_dQ^{-1}$, where P_d is the perspective projection matrix defined in Definition III.1.

C. Rendering process

Let renderable objects be located in a domain Ω. We aim to simplify the scene by dividing Ω into m disjoined parts Ω_i called *cells*, replacing each with a planar representation of their contained objects. These so-called *impostors*, will be created for the same initial viewport(s), that is, for a certain viewport we will create an *impostor set* with one impostor per cell, all for that particular viewport. This will be done for n initial viewports resulting in n impostor sets with m impostors each.

As long as the current viewport matches the initial viewport for which the impostors have been created, the impostor representation coincides with the image of the actual scene. Changing the viewport, however, will introduce parallax errors, since depth information has been lost in the impostor creation process.

To determine this error, we will first regard a single cell Ω_i and a single vertex $v \in \Omega_i$. For a fixed initial viewport χ_1 we calculate the impostor representation $\overline{v}$ of the actual point v. Then we assume changing to another variable viewport χ and calculate the screen coordinates v' of v and $\overline{v}'$ of $\overline{v}$ as functions of the viewports χ and χ_1 (cf. Figure III.2).

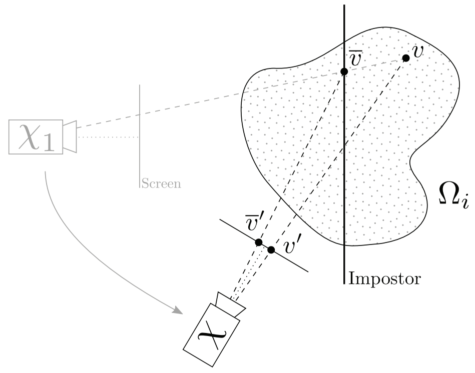

Figure III.2. Rendering process for changed viewport

D. The domain error

For every point in Ω, if we perform the procedure above, we obtain two images. One image of itself (v', depending on χ) and one of its impostor representation ($\overline{v}'$, depending on both χ and χ_1). The screen distance of these two, measured in (sub-)pixels is called the *screen space error*. As we are hardly interested in the error of a single point, but rather in error functions expressing the error of the entire scene, for example the mean error or the maximum error, we aggregate the screen space error over all point in Ω. As the distribution of vertices inside Ω is supposed to be unknown, we assume a uniform distribution and integrate the screen space error over the entire domain Ω. We will be using the maximum error which replaces the integral with a supremum.

Definition III.4. Denote the number of cells with m. For an initial viewport χ_1 we define the *domain error*

$$\begin{aligned} \mathrm{D}(\chi, \chi_1) \quad &:= \quad \sup_{v \in \Omega} \left\| v'(\chi) - \overline{v}'(\chi, \chi_1) \right\|_2 \\ &= \quad \max_{0 \le i \le m} \left\{ \sup_{v \in \Omega_i} \left\| v'(\chi) - \overline{v}'(\chi, \chi_1) \right\|_2 \right\}. \end{aligned}$$

This domain error depends on a variable observer viewport χ and a fixed viewport χ_1, for which the displayed impostors have been initially created. Dependence on χ implies, that we can not evaluate our impostor approximation without knowledge of the observer movement. Clearly, we want to optimize our setup a priory for what reason we need to find a way to evaluate it without knowledge of χ.

E. The interaction error

Assume we have n impostor sets at hand for viewports $\chi_1, \ldots, \chi_n \in \Lambda \subset X$ and, as before, denote the observer's viewport with $\chi \in \Lambda$. Since we can choose from several impostor sets, we display that set whose initial impostor χ_k satisfies

$$\mathrm{D}_p(\chi, \chi_k) = \min_{1 \le j \le n} \mathrm{D}_p(\chi, \chi_j).$$

For $1 \leq k \leq n$ let Ξ_k denote that subset of Λ, on which $\mathrm{D}_p(\chi, \chi_k)$ is the smallest of all domain errors, that is,

$$\Xi_k := \big\{ \chi \in \Lambda \,\big|\, \mathrm{D}_p(\chi, \chi_k) = \min_{1 \leq j \leq n} \mathrm{D}_p(\chi, \chi_j) \big\}. \quad \text{(III.1)}$$

Next, we define a probability distribution P with an associated probability density function μ on Λ, for instance, a uniform distribution over Λ or a normal distribution around the current viewport χ. These distributions represent the probability for the respective viewport "to happen", thus modeling the expected observer movement. We can then calculate the expected value of the error by integrating the domain error D_p over Λ with respect to the probability distribution P.

Definition III.5. Let $n \geq 1$. We define the *interaction error* $\mathrm{I}_p : \Lambda^n \to \mathbb{R}$, where

$$\begin{aligned} \mathrm{I}_p(\chi_1, \ldots, \chi_n) &:= \int_\Lambda \min_{1 \leq j \leq n} \mathrm{D}_p(\chi, \chi_j)\, \mathrm{d}P(\chi) \quad \text{(III.2)} \\ &= \sum_{j=1}^{n} \int_{\Xi_j} \mathrm{D}_p(\chi, \chi_j)\, \mathrm{d}P(\chi). \end{aligned}$$

We expect that the interaction error will decrease as we add more viewports. We prove this assumption in

Lemma III.6. Let $\chi_1, \ldots, \chi_n \in \Lambda$. Then

$$\mathrm{I}_p(\chi_1) \geq \mathrm{I}_p(\chi_1, \chi_2) \geq \cdots \geq \mathrm{I}_p(\chi_1, \ldots, \chi_n).$$

Proof: For $1 \leq k \leq n$, it is

$$\begin{aligned} \mathrm{I}_p(\chi_1, \ldots, \chi_k) &= \int_\Lambda \min_{1 \leq j \leq k} \mathrm{D}_p(\chi, \chi_j)\, \mathrm{d}P(\chi) \\ &\leq \int_\Lambda \min_{1 \leq j \leq k-1} \mathrm{D}_p(\chi, \chi_j)\, \mathrm{d}P(\chi) \\ &= \mathrm{I}_p(\chi_1, \ldots, \chi_{k-1}). \end{aligned}$$

■

IV. Impostor placement and error bounds

The efficiency of the proposed method is based on an optimal choice of initial viewports for the impostor sets, as well as an optimized cell partition for each set.

Theorem IV.1. Given renderable objects located in

$$\Omega := \big\{ (x_1, x_2, x_3, 1)^\top \in \mathbb{P}^3 \,\big|\, 0 < a_0 < x_3 < a_{m+1} \leq \infty \big\},$$

the optimal cell boundaries for viewport translations are given by $a_i = (1/a_0 - \delta i)^{-1}$, $i = 1, \ldots, m$ for a suitable $\delta(m) > 0$, and the optimal impostor placement with respect to the error metrics is

$$d_i = \frac{2 a_i a_{i+1}}{a_i + a_{i+1}}.$$

Note, that m is finite even for domains with infinite depth, that is, when $a_{m+1} = \infty$ for which $d_m = 2a_m$.

Proof: For viewport translations the minimum of the domain error D with respect to the projection plane distance $d \in [a, b]$ can be found analytically. For details see [15, Theorem 3.2]. ■

With this impostor placement, we have the following error asymptotics with respect to viewport translations:

Theorem IV.2. For a fixed maximal screen space error $\varepsilon > 0$, the radius r of maximal permissible viewport change is proportional to the number of impostors per set m.

Proof: This property emerges during the proof of Theorem IV.1. For details see [15, Remark 3.5]. ■

This Theorem shows, that increasing the number of impostors per set will strongly decrease the interaction error, but the number of displayable impostors is bound by the graphical capabilities of mobile devices. Due to such limitations, several impostors sets have to be transmitted.

Denote the number of impostor sets with n. Under certain assumptions we can show that the inspection error can be bounded by

$$C_1 n^{-1/5} \leq \mathrm{I}(\chi_1, \ldots, \chi_n) \leq C_2 n^{-1/5},$$

for constants $C_{1/2} = C_{1/2}(\Lambda, m)$. Proofing these bounds will be the endeavor of the next section.

V. Model evaluation

Proposition V.1. Using the $\mathbb{R}^5$-parametrization of the viewport space, we can regard the domain error $\mathrm{D}(\chi, \chi_k)$ as a continuous function $f : \mathbb{R}^5 \times \mathbb{R}^5 \to \mathbb{R}$ which, for moderate viewport changes, behaves almost linear. More precisely, we can find positive constants $a_1, \ldots a_5$ and $\bar{a}_1, \ldots, \bar{a}_5$ such that

$$\|A_1(x-y)\| \leq f(x, y) \leq \|A_2(x-y)\| \quad \text{(V.1)}$$

where $A_1 := \operatorname{diag}(a_1, \ldots, a_5)$ and $A_2 := \operatorname{diag}(\bar{a}_1, \ldots, \bar{a}_5)$.

Proposition V.2. The matrices A_1 and A_2 depend on the number of cells m. For viewport translations they are proportional to m^{-1} as a direct consequence of Theorem IV.2.

Before proceeding, we need the following Lemmata.

Remark V.3. In the following $A = B + C$ means that the set A is the direct sum of the sets B and C, that is, $A = B \cup C$ and $B \cap C = \emptyset$. In particular, $\operatorname{vol}(A + B) = \operatorname{vol}(A) + \operatorname{vol}(B)$.

Similarly, $A = B - C$ means that $B = A + C$, that is, $C \subset B$ and $\operatorname{vol}(B - C) = \operatorname{vol}(B) - \operatorname{vol}(C)$.

Lemma V.4. Let G be a bounded, measurable, d-dimensional subset of $\mathbb{R}^d$ and let B be a d-dimensional ball (with respect to a norm $\|\cdot\|$) of equal volume (cf. Figure V.1a). Then

$$\int_G \|x\|\, \mathrm{d}x \;\geq\; \int_B \|x\|\, \mathrm{d}x.$$

Proof: Denote the radius of B with R. Due to $G = G \cap B + G \backslash B$ and $B = G \cap B + B \backslash G$, we can express G as

$G = (B - B\backslash G) + G\backslash B$. As the volumes of G and B are equal, this also implies $\mathrm{vol}\,(G\backslash B) = \mathrm{vol}\,(B\backslash G)$. Moreover, all points in $G\backslash B$ have a radius larger than R and all points in $B\backslash G$ have a radius smaller than R. Hence,

$$\int_{G\backslash B} \|x\| \,\mathrm{d}x \geq \int_{G\backslash B} R \,\mathrm{d}x = R\,\mathrm{vol}\,(G\backslash B)$$

and, conversely,

$$\int_{B\backslash G} \|x\| \,\mathrm{d}x \leq \int_{B\backslash G} R \,\mathrm{d}x = R\,\mathrm{vol}\,(B\backslash G)\,.$$

This implies

$$\begin{aligned}\int_G \|x\| \,\mathrm{d}x &= \int_B \|x\| \,\mathrm{d}x - \int_{B\backslash G} \|x\| \,\mathrm{d}x + \int_{G\backslash B} \|x\| \,\mathrm{d}x \\ &\geq \int_B \|x\| \,\mathrm{d}x - R\underbrace{\big(\mathrm{vol}\,(B\backslash G) - \mathrm{vol}\,(G\backslash B)\big)}_{=0}.\end{aligned}$$

■

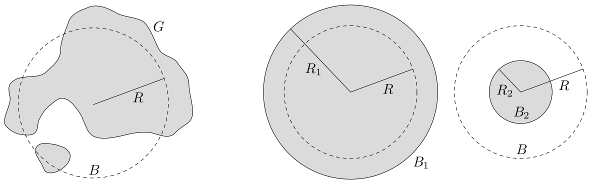

(a) Lemma V.4. (b) Lemma V.5.

Figure V.1. Accompanying illustrations for the lemmata.

Lemma V.5. Let B and $B_1, \ldots, B_n$ be d-dimensional balls (with respect to a norm $\|\cdot\|$), such that the volume of B is the arithmetic mean of the volumes of $B_1, \ldots, B_n$. Then

$$\sum_{k=1}^{n} \int_{B_k} \|x\| \,\mathrm{d}x \;\geq\; n \int_B \|x\| \,\mathrm{d}x.$$

Proof: We first regard the case $n = 2$. Without loss of generality, let $R_1 \geq R \geq R_2$.

We define $G := (B_1 - B) + B_2$. Then, $\mathrm{vol}\,(G) = \mathrm{vol}\,(B_1) - \mathrm{vol}\,(B) + \mathrm{vol}\,(B_2) = \mathrm{vol}\,(B)$ and Lemma V.4 yields

$$\begin{aligned}\int_B \|x\| \,\mathrm{d}x &\leq \int_G \|x\| \,\mathrm{d}x \\ &= \int_{B_1} \|x\| \,\mathrm{d}x - \int_B \|x\| \,\mathrm{d}x + \int_{B_2} \|x\| \,\mathrm{d}x.\end{aligned}$$

From this, the general case follows by induction. ■

Lemma V.6. Let B be a 5-dimensional ball with radius R. Then

$$\int_B \|x\|_2 \,\mathrm{d}x \;=\; \frac{4}{9}\pi^2 R^6.$$

Proof: Straightforward calculation using 5-dimensional polar coordinates. ■

With these Lemmata, we can proof the following estimation to the inspection error:

Theorem V.7. Let Λ be bounded and assume a uniform distribution. Then, the interaction error can be bounded from below by

$$\mathrm{I}(\chi_1, \ldots, \chi_n) \;\geq\; C_1 n^{-1/5},$$

with the constant

$$C_1 := \frac{5}{6}\left(\frac{15}{8\pi^2}\det(A_1)\mathrm{vol}\,(\Lambda)\right)^{1/5},$$

where $A_1 := \mathrm{diag}(a_1, \ldots, a_5)$ with constants $a_i > 0$ as in Proposition V.1.

Proof: Let us first recall (III.1) and (III.2). Assuming a uniform distribution $\mu(\chi) = \mathrm{vol}\,(\Lambda)^{-1}$ we can rewrite (III.2) as

$$\mathrm{I}(\chi_1, \ldots, \chi_n) = \mathrm{vol}\,(\Lambda)^{-1} \sum_{k=1}^{n} \int_{\Xi_k} \mathrm{D}(\chi, \chi_k) \,\mathrm{d}\chi. \quad \text{(V.2)}$$

On the right-hand side, we have to evaluate n integrals of the form $\int_G f(x,y)\,dx$. Using (V.1) we define a transformation of coordinates $\Phi(x) := A_1(x - y)$ (which is the same for all n integrals!) and obtain

$$\int_G f(x,y)\,dx \;\geq\; \int_G \|\Phi(x)\| \,\mathrm{d}x \;=\; \frac{1}{\det(A_1)} \int_{\Phi(G)} \|x\| \,\mathrm{d}x.$$

Applying this to (V.2) yields

$$\mathrm{I}(\chi_1, \ldots, \chi_n) \geq (\det(A_1)\mathrm{vol}\,(\Lambda))^{-1} \sum_{k=1}^{n} \int_{\Phi_k(\Xi_k)} \|x\| \,\mathrm{d}x. \quad \text{(V.3)}$$

Using Lemmata V.4 and V.5 (with $d = 5$) we obtain

$$\sum_{k=1}^{n} \int_{\Phi_k(\Xi_k)} \|x\| \,\mathrm{d}x \geq \sum_{k=1}^{n} \int_{B_k} \|x\| \,\mathrm{d}x \geq n \int_B \|x\| \,\mathrm{d}x,$$

where

$$\begin{aligned}\mathrm{vol}\,(B) &= \frac{1}{n}\sum_{k=1}^{n}\mathrm{vol}\,(B_k) = \frac{1}{n}\sum_{k=1}^{n}\mathrm{vol}\,(\Phi_k(\Xi_k)) \\ &= \frac{1}{n}\det(A_1)\mathrm{vol}\,(\Lambda)\,. \quad \text{(V.4)}\end{aligned}$$

With this, we can continue with our estimation (V.3) and obtain

$$\mathrm{I}(\chi_1, \ldots, \chi_n \geq (\det(A_1)\mathrm{vol}\,(\Lambda))^{-1}\, n \int_B \|x\| \,\mathrm{d}x$$

Now, we choose to use the Euclidean norm $\|\cdot\| = \|\cdot\|_2$ for which a 5-dimensional ball with radius R has the volume $\mathrm{vol}\,(B) = \frac{8}{15}\pi^2 R^5$. Then, (V.4) implies

$$R = \left(\frac{15}{8n\pi^2}\det(A_1)\mathrm{vol}\,(\Lambda)\right)^{1/5}.$$

Hence, using Lemma V.6,

$$\int_B \|x\|\,\mathrm{d}x = \frac{5}{6n}\det(A_1)\mathrm{vol}\,(\Lambda)\left(\frac{15}{8n\pi^2}\det(A_1)\mathrm{vol}\,(\Lambda)\right)^{1/5}.$$

Inserting this into (V) we finally obtain

$$\mathrm{I}(\chi_1,\ldots,\chi_n) \;\geq\; \frac{5}{6}\left(\frac{15}{8n\pi^2}\det(A_1)\mathrm{vol}\,(\Lambda)\right)^{1/5}.$$

■

This Theorem has proven, that the efficiency of any choice of impostor sets can not be better than the given estimate. The following Theorem constructively proves, that a choice of impostor sets with the desired asymptotics exists, that is, that this estimate is actually achievable.

Theorem V.8. Let Λ be bounded with a uniform distribution and let $\tilde{\Lambda} \supset \Lambda$ be an enclosing cuboid. Then, there is a set of viewports $\chi_1, \ldots \chi_n$ for which the interaction error satisfies

$$\mathrm{I}(\chi_1,\ldots,\chi_n) \;\leq\; C_2 n^{-1/5},$$

with the constant

$$C_2 := \frac{\pi^2}{36}\frac{(\max\{\bar{a}_1,\ldots,\bar{a}_5\}\mathrm{diam}(\tilde{\Lambda}))^6}{\det(A_2)\mathrm{vol}\,(\Lambda)},$$

where $A_2 := \mathrm{diag}(\bar{a}_1,\ldots,\bar{a}_5)$ with constants $\bar{a}_i > 0$ as in Proposition V.1.

Proof: To begin with, we will proof the assertion for those n which are the fifth power of a whole number, that is, for $n^{1/5} \in \mathbb{N}$. The general case will be derived from this case later.

First, a bounded Λ can be embedded into a cuboid $\tilde{\Lambda}$. For an n as above, there is a regular decomposition of $\tilde{\Lambda}$ into five-dimensional cuboids Ξ_k with initial viewports χ_k at their respective centers.

Using the estimation $f(x,y) \leq \|A_2(x-y)\| = \|\Psi(x)\|$ with the same arguments as in the proof of Theorem V.7, we obtain

$$\begin{aligned}\mathrm{I}(\chi_1,\ldots,\chi_n) &\leq \mathrm{vol}\,(\Lambda)^{-1}\sum_{k=1}^{n}\int_{\Xi_k}\mathrm{D}(\chi,\chi_k)\,\mathrm{d}\chi\\ &\leq (\det(A_2)\mathrm{vol}\,(\Lambda))^{-1}\sum_{k=1}^{n}\int_{\Psi_k(\Xi_k)}\|x\|\,\mathrm{d}x\\ &\leq (\det(A_2)\mathrm{vol}\,(\Lambda))^{-1}\,n\int_B\|x\|\,\mathrm{d}x, \qquad \text{(V.5)}\end{aligned}$$

where, in the last step, we used that all cuboids $\Psi_k(\Xi_k)$ are identical and can be embedded into a ball B. For this the radius needs to be at least

$$R = \frac{1}{2}\mathrm{diam}(\Psi_k(\Xi_k)) \geq \max\{\bar{a}_1,\ldots,\bar{a}_5\}\frac{\mathrm{diam}(\tilde{\Lambda})}{2n^{1/5}}.$$

With this and Lemma V.6 we finally obtain from (V.5)

$$\mathrm{I}(\chi_1,\ldots,\chi_n) \;\leq\; \frac{\pi^2}{72}\frac{(\max\{\bar{a}_1,\ldots,\bar{a}_5\}\mathrm{diam}(\tilde{\Lambda}))^6}{\det(A_2)\mathrm{vol}\,(\Lambda)}n^{-1/5}.$$

Now, for the general case, we divide $\tilde{\Lambda}$ into $\tilde{n} := \lfloor n^{1/5}\rfloor^5 \leq n$ cubes. This is possible because $\tilde{n}$ is the fifth power of a whole number ($\tilde{n}^{1/5} \in \mathbb{N}$). Moreover,

$$\frac{\tilde{n}^{-1/5}}{n^{-1/5}} = \frac{n^{1/5}}{\lfloor n^{1/5}\rfloor} \leq \frac{\lfloor n^{1/5}\rfloor + 1}{\lfloor n^{1/5}\rfloor} = 1 + \frac{1}{\lfloor n^{1/5}\rfloor} \leq 2,$$

that is, $\tilde{n}^{-1/5} \leq 2n^{-1/5}$. Hence, by this and Lemma (III.6)

$$\begin{aligned}\mathrm{I}(\chi_1,\ldots,\chi_n) &\leq I(\chi_1,\ldots,\chi_{\tilde{n}})\\ &\leq \frac{\pi^2}{72}\frac{(\max\{\bar{a}_1,\ldots,\bar{a}_5\}\mathrm{diam}(\tilde{\Lambda}))^6}{\det(A_2)\mathrm{vol}\,(\Lambda)}\tilde{n}^{-1/5}\\ &\leq \frac{\pi^2}{36}\frac{(\max\{\bar{a}_1,\ldots,\bar{a}_5\}\mathrm{diam}(\tilde{\Lambda}))^6}{\det(A_2)\mathrm{vol}\,(\Lambda)}n^{-1/5}.\end{aligned}$$

■

Remark V.9. As stated earlier, the matrices A_1, A_2 depend on the number of cells m. With the assumptions in Proposition V.2, it follows that $\mathrm{I} = \mathcal{O}(m^{-1}n^{-1/5})$.

VI. Conclusion

In this text, we developed a mathematical model which allows to measure, analyze and optimize the display error of image-based approximation techniques. The error asymptotics derived for our method based on parallelized rendering shows a clear advantage over traditional remote visualization concepts like Virtual Network Computing (VNC) which, under ideal conditions, represent the scene by one image $m = 1$. In contrast to this, $m = 10$ impostors with $n = 1$ viewport cover the same volume of permissible viewports, as $m = 1$ impostors for $n = 10000$ optimally chosen viewport sets. Considering the bandwidth $\mathcal{O}(mn)$ needed for transmission of impostors compared with the error contribution $\mathcal{O}(m^{-1}n^{-1/5})$, the method offers significant decrease of bandwidth consumption, and low latency rendering for the user.

The proposed method strongly benefits from graphical capabilities of clients, such as mobile devices, and will increase its efficiency for each new generation providing increased graphical performance. Due to the parallelization of server-sided image generation, and the proven efficiency thereof, the method is applicable to large and distributed data sets for visualization on mobile devices and thin clients.

Acknowledgement

The authors appreciate the support of the 'Federal Ministry of Education and Research' and 'Eurostars' within the Project E! 5643 MobileViz. The Eurostars Project is funded by the European Union.

References

[1] S. Jeschke, M. Wimmer, and W. Purgathofer, "Star: Image-based representations for accelerated rendering of complex scenes," *Proc. of Eurographics*, 2005.

[2] H.-Y. Shum and S. B. Kang, "A review of image-based rendering techniques," in *IEEE/SPIE Visual Communications and Image Processing*, 2000.

[3] S. Jeschke and M. Wimmer, "An error metric for layered environment map impostors," Tech. Rep. TR-186-2-02-04, 2002.

[4] S. Jeschke, M. Wimmer, and H. Schuman, "Layered environment-map impostors for arbitrary scenes," *Graphics Interface*, May 2002.

[5] W.-C. Wang, K.-Y. Li, X. Zheng, and E.-H. Wu, "Layered textures for image-based rendering," *Journal of Computer Science and Technology*, vol. 19, no. 5, pp. 633–642, September 2004.

[6] M. Moser and D. Weiskopf, "Interactive volume rendering on mobile devices," in *13th Fall Workshop: Vision, modeling, and visualization 2008*, O. Deussen, D. Keim, and D. Saupe, Eds. Akademische Verlagsgesellschaft AKA GmbH, 2008, p. 217.

[7] J. Cohen, D. Manocha, and M. Olano, "Simplifying polygonal models using successive mappings," in *VIS '97: Proceedings of the 8th conference on Visualization '97*. Los Alamitos, CA, USA: IEEE Computer Society Press, 1997, p. 395ff.

[8] P. Debevec, Y. Yu, and G. Boshokov, "Efficient view-dependent image-based rendering with projective texture-mapping," Berkeley, CA, USA, Tech. Rep., 1998.

[9] J. Kopf, B. Chen, R. Szeliski, and M. Cohen, "Street slide: browsing street level imagery," *ACM Trans. Graph.*, vol. 29, no. 4, pp. 1–8, 2010.

[10] J. Shade, D. Lischinski, D. H. Salesin, T. DeRose, and J. Snyder, "Hierarchical image caching for accelerated walk-throughs of complex environments," in *SIGGRAPH '96: Proceedings of the 23rd annual conference on Computer graphics and interactive techniques*. New York, NY, USA: ACM, 1996, pp. 75–82.

[11] T. A. Funkhouser, "Database management for interactive display of large architectural models," in *GI '96: Proceedings of the conference on Graphics interface '96*. Toronto, Ont., Canada, Canada: Canadian Information Processing Society, 1996, pp. 1–8.

[12] M. Hoffmann and J. Kohlhammer, "A generic framework for using interactive visualization on mobile devices," *Communications in Computer and Information Sciene*, vol. 53, no. 4, pp. 131–142, 2009.

[13] F. Lamberti, C. Zunino, A. Sanna, A. Fiume, and M. Maniezzo, "An accelerated remote graphics architecture for pdas," in *Web3D '03: Proceedings of the eighth international conference on 3D Web technology*. New York, NY, USA: ACM, 2003, p. 55ff.

[14] A. Beutelspacher and U. Rosenbaum, *Projective Geometry: From Foundations to Applications*. Cambridge University Press, February 1998.

[15] R. Reiner, "Numerical methods for optimal impostor prefetching in scientific visualization," Diploma Thesis, Karlsruhe Institute of Technology, 2011.

Preprint Series of the Engineering Mathematics and Computing Lab

recent issues

No. 2012-06 Thomas Henn, Vincent Heuveline, Mathias J. Krause, Sebastian Ritterbusch: Aortic Coarctation simulation based on the Lattice Boltzmann method: benchmark results

No. 2012-05 Vincent Heuveline, Eva Ketelaer, Staffan Ronnas, Mareike Schmidtobreick, Martin Wlotzka: Scalability Study of HiFlow^3 based on a Fluid Flow Channel Benchmark

No. 2012-04 Hartwig Anzt, Armen Beglarian, Suren Chilingaryan, Andrew Ferrone, Vincent Heuveline, Andreas Kopmann: A unified Energy Footprint for Simulation Software

No. 2012-03 Vincent Heuveline, Chandramowli Subramanian: The Coffee-table Book of Pseudospectra

No. 2012-02 Dominik P.J. Barz, Hendryk Bockelmann, Vincent Heuveline: Electrokinetic optimization of a micromixer for lab-on-chip applications

No. 2012-01 Sven Janko, Björn Rocker, Martin Schindewolf, Vincent Heuveline, Wolfgang Karl: Software Transactional Memory, OpenMP and Pthread implementations of the Conjugate Gradients Method - a Preliminary Evaluation

No. 2011-17 Hartwig Anzt, Jack Dongarra, Vincent Heuveline, Piotr Luszczek: GPU-Accelerated Asynchronous Error Correction for Mixed Precision Iterative Refinement

No. 2011-16 Vincent Heuveline, Sebastian Ritterbusch, Staffan Ronnås: Augmented Reality for Urban Simulation Visualization

No. 2011-15 Hartwig Anzt, Jack Dongarra, Mark Gates, Stanimire Tomov: Block-asynchronous multigrid smoothers for GPU-accelerated systems

No. 2011-14 Hartwig Anzt, Jack Dongarra, Vincent Heuveline, Stanimire Tomov: A Block-Asynchronous Relaxation Method for Graphics Processing Units

No. 2011-13 Vincent Heuveline, Wolfgang Karl, Fabian Nowak, Mareike Schmidtobreick, Florian Wilhelm: Employing a High-Level Language for Porting Numerical Applications to Reconfigurable Hardware

No. 2011-12 Vincent Heuveline, Gudrun Thäter: Proceedings of the 4th EMCL-Workshop Numerical Simulation, Optimization and High Performance Computing

No. 2011-11 Thomas Gengenbach, Vincent Heuveline, Mathias J. Krause: Numerical Simulation of the Human Lung: A Two–scale Approach

No. 2011-10 Vincent Heuveline, Dimitar Lukarski, Fabian Oboril, Mehdi B. Tahoori, Jan-Philipp Weiss: Numerical Defect Correction as an Algorithm-Based Fault Tolerance Technique for Iterative Solvers

No. 2011-09 Vincent Heuveline, Dimitar Lukarski, Nico Trost, Jan-Philipp Weiss: Parallel Smoothers for Matrix-based Multigrid Methods on Unstructured Meshes Using Multicore CPUs and GPUs

The responsibility for the contents of the working papers rests with the authors, not the Institute. Since working papers are of a preliminary nature, it may be useful to contact the authors of a particular working paper about results or caveats before referring to, or quoting, a paper. Any comments on working papers should be sent directly to the authors.